Published in IEEE Photonics Journal 12, issue 2, p.1-9, Art no. 1500609, 2020
which should be used for any reference to this work

Carrier-Envelope Offset Frequency Stabilization of a Thin-Disk Laser Oscillator via Depletion Modulation

José R. C. Andrade,[1,2] **Norbert Modsching**,[3] **Ayhan Tajalli**,[1,2] **Christian M. Dietrich**,[1,2] **Sven Kleinert**,[1,2] **Fabian Placzek**,[1] **Bernhard Kreipe**,[1] **Stephane Schilt**,[3] **Valentin J. Wittwer**,[3] **Thomas Südmeyer**,[3] ***Member, IEEE***, **and Uwe Morgner**[1,2]

[1]Institute of Quantum Optics, Leibniz Universität Hannover, 30167 Hannover, Germany
[2]Cluster of Excellence PhoenixD (Photonics, Optics, and Engineering – Innovation Across Disciplines), 30167 Hannover, Germany
[3]Laboratoire Temps-Fréquence (LTF), Institut de Physique, Université de Neuchâtel, 2000 Neuchâtel, Switzerland

DOI:10.1109/JPHOT.2020.2970858

Manuscript received December 20, 2019; revised January 27, 2020; accepted January 29, 2020. Date of publication January 31, 2020; date of current version March 9, 2020. This work was supported in part by Deutsche Forschunggemeinschaft (DFG) under projects MO 850-19/2 and MO 850-20/1 as well as Germany's Excellence Strategy within the Cluster of Excellence PhoenixD EXC 2122, Project ID 390833453 and in part by Swiss National Science Foundation (SNSF) (200020_179146).
Corresponding author: José R. C. Andrade (e-mail: andrade@iqo.uni-hannover.de).

Abstract: We present a novel concept for the stabilization of the carrier-envelope offset (CEO) frequency of femtosecond pulse trains from thin-disk laser oscillators by exploiting gain depletion modulation in the active gain region. We shine a small fraction of the laser output power back onto the thin disk allowing the population inversion in the gain medium to be controlled. We employ this technique in our home-built Kerr-lens mode-locked Yb:YAG thin-disk laser and benchmark the performance against the proven technique of pump current modulation for CEO stabilization, showing that the two techniques have equivalent performance. The new method which only requires an additional AOM demonstrates a scalable and cost-effective method for CEO stabilization of high-power laser oscillators.

Index Terms: Ultrafast oscillators, CEO stabilization.

1. Introduction

In the past decade, technologies based on ultrafast thin-disk (TDL) laser oscillators have seen a steady scalability of the achieved average power into the hundreds of watts [1], [2] and peak powers beyond 150 MW [2]. Post compression of the pulses of these oscillators down to the few-cycle regime was also demonstrated [3], [4] which is a key parameter for several applications [5].

As materials mature, and TDLs scale further – decrease in complexity, higher peak powers, shorter pulse durations, and their eventual frequency conversion to other spectral ranges through nonlinear processes – the necessity of controlling the features of the electromagnetic field at its fundamental level is paramount. In the case of high-field science, stabilization of the carrier-envelope phase to an abitrary value usually suffices. Spectroscopic applications relying on frequency combs [6], [7], however, generally require the stabilization of both the repetition rate of the system (f_{rep}) and carrier-envelope offset frequency (f_{CEO}) [8]. Control of the f_{rep} can be done by

a servo loop actuating on a cavity mirror mounted on a piezo actuator. In contrast, f_{CEO} stabilization requires more sophisticated detection and control schemes. A coherent octave-spanning spectrum is required for the self-referenced f_{CEO} detection in an $f-2f$ interferometer [8], [9]. Short pulse durations, typically in the range of $<$150 fs, are needed to generate such a spectrum in highly nonlinear fibers, longer pulses resulting in a degraded coherence [10]. Reported high-power systems rely on external nonlinear pulse compression before the generation of a supercontinuum spectrum. TDLs delivering pulses below 150 fs, albeit with less output power, can directly drive this process [10]–[14]. After f_{CEO} detection, stabilization of this parameter in TDLs has been mainly done via modulation of the pump power. This was realized either by using a dedicated electronic module (voltage-to-current converter) placed in parallel to the high current DC source for direct modulation of the pump diode [11]–[13], or by the dichroic combination of a second low-power pump diode with fast modulation capabilities to avoid the modulation of high currents at high frequencies [15]. However, the former requires electronics which are not commercially available and the latter, besides using an in-house coated dichroic mirror, manipulates the pump beam path, which might be detrimental at high pump powers.

Another demonstrated method for CEO stabilization of TDLs employs an acousto-optic modulator (AOM) in the oscillator [3], [16] enabling a direct modulation of the intracavity losses. This scheme proved to be power-scalable and allowed the realization of a tight CEO lock due to a large locking bandwidth of 230 kHz. In the work of Gröbmeyer *et al.* [16], the AOM was used as the Kerr-lens element of the TDL and the laser output power exceeded 100 W. However, a special AOM was needed, and with the advent of more sophisticated designs for high-power TDLs [17], the inclusion of an intracavity AOM might be hindered in the future.

Lastly, worthy of consideration for the stabilization of TDLs is the use of a semiconductor saturable absorber mirror (SESAM) as an opto-optical modulator [18]. Other methods for f_{CEO} locking in the case of high-power TDLs have been discussed elsewhere [16].

In this Article, we present a different scheme for the CEO stabilization of TDLs based on modulating the gain of the thin disk by illuminating it with a small fraction of the laser output power itself. In this way, the only additional needed element besides the stabilization electronics for locking f_{CEO} is an AOM without particular requirements. We demonstrate a similar performance compared to the standard pump current modulation. Furthermore, the octave-spanning spectrum needed for the CEO beat detection is generated in a bulk medium [19] instead of using a highly-nonlinear fiber. Here, the alignment procedure is simpler and with less optical components, but relies on multi-MW peak powers to drive the process.

2. Experimental Setup and Results

A sketch of the experimental setup is shown in Fig. 1. Our home-built Kerr-lens mode-locked (KLM) Yb:YAG TDL has a repetition rate of 33 MHz and uses a 3 mm fused silica plate as the Kerr-lens element and an output coupler with a transmission of 15%. The oscillator emits 0.85 μJ solitonic pulses with a duration of 275 fs centered at a wavelength of 1032 nm resulting in an average output power of 28 W. Two fractions of the laser output power are used for the detection (5.7 W) and stabilization ($<$3 W) of the CEO frequency. The 5.7 W are launched into a 5.6 cm-long large mode area fiber (NKT Photonics LMA-25) to produce sub-40-fs pulses after a prism compressor, with an overall efficiency of 68%. In the case of our supercontinuum spectrum generation (SCG) in YAG, the critical power for self-focusing is 1.25 MW. Although the output power of our system is sufficient to reach this level, the required average power ($>$12 W) leads to damage, while also substantially decreasing the useful power of the system. Therefore, we drove the process after a single compression stage, greatly reducing the needed energy for SCG and resulting in a stable supercontinuum spectrum from an undoped 4 mm thick YAG plate. The supercontinuum light is then launched into a Michelson-type $f-2f$ interferometer. The detected CEO beat signal has a signal-to-noise ratio of 35–40 dB at a resolution bandwidth of 100 kHz. The other fraction of the laser output power of $<$3 W passes through the telescope T1 to adapt the beam size to the clear apertures of an AOM (AA Opto-Electronic QCQ40-A2.5-L1064-Z42-C35Sa) and an isolator. The

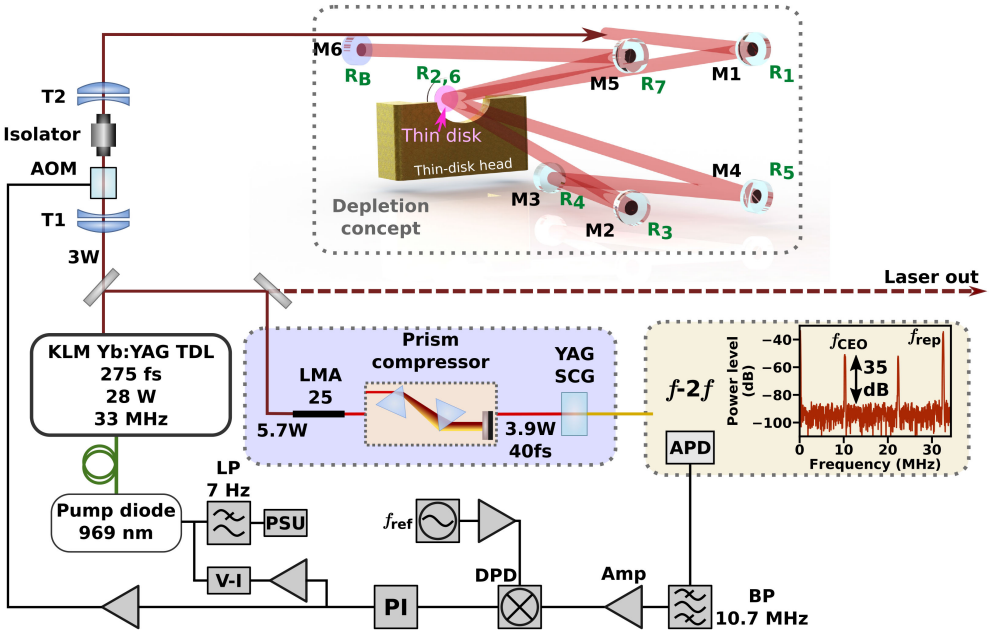

Fig. 1. Conceptual setup of the stabilization scheme for the KLM Yb:YAG TDL. Electrical connections are drawn as black lines and optical beams in color. T1, T2, telescopes; M1-M6, highly-reflective mirrors with the numbered reflections as subscript of R; APD, avalanche photo-diode; BP, bandpass filter; LP, low-pass filter; DPD, digital phase detector; PSU, power supply unit; V-I, voltage-to-current converter; Amp, amplifier; SCG, supercontinuum generation; LMA, large mode area fiber; PI, proportional-integral servo. Details of the setup are given in the text. The displayed RF spectrum of f_{CEO} has a resolution bandwidth of 100 kHz.

second telescope T2 adapts the beam for its imaging on the thin disk. The beam is then folded up to four times on the pumped region of the thin disk, exploiting the accessible solid angle. The upper panel of Fig. 1 shows the concept of the depletion beam-path, steered by six highly reflective mirrors (M1-M6), where M6 is back reflecting. The folded beam acts as a depletion channel for the ions in the upper laser level by stimulated emission. The higher the power of this beam, the stronger the depletion of the population inversion of the gain medium. Modulating the incident beam power modulates in opposite phase the gain seen by the intracavity beam. For the stabilization of the detected CEO frequency, the signal is first band-pass filtered at 10.7 MHz and amplified (MenloSystems OFD80) before being fed into a digital phase detector (MenloSystems DXD200) where it is compared in phase to a reference radio-frequency (RF) signal f_{ref}. The resulting error signal is amplified in a proportional-integral servo controller (MenloSystems PIC201) and the feedback signal is applied either to a voltage-to-current (V-I) converter to modulate the current of the pump diode, to the AOM modulating the power of the 3 W beam shining onto the disk, or to both simultaneously. The home-designed V-I converter (same one as used in [13], with an electrical modulation bandwidth of 1 MHz) is connected to the wavelength-stabilized 969 nm pump diode in parallel to a high DC power supply unit (PSU). A 7 Hz low-pass filter prevents cross-talk between the V-I converter and PSU [13]. The coarse control of f_{CEO} is done via a pair of fused silica wedges, inserted at Brewester's angle into the laser cavity [20].

2.1 Frequency Response

With this setup, the transfer function of the TDL output power was measured under different conditions using a lock-in amplifier (SRS SR865 A) as displayed in Fig. 2. For pump power modulation applied to the laser operating in continuous-wave (CW) at the same pump power level

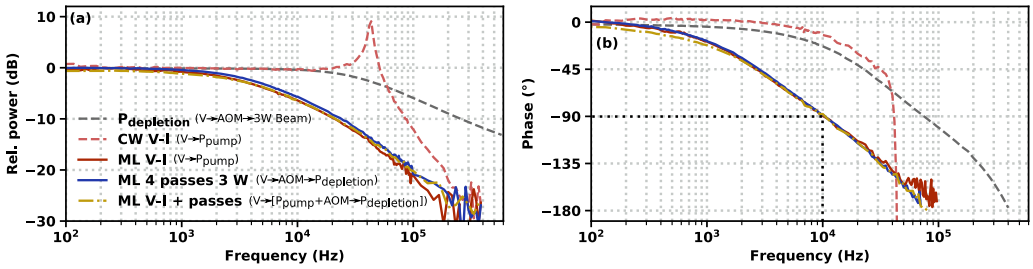

Fig. 2. Bode plot of the different components of the system. (a) Relative amplitude response, (b) phase lag/lead. The transfer function of the 3 W control beam power by the AOM is shown in dashed grey. The red curves show the response of the laser output power in CW (dashed) and mode-locked (ML) operation (solid) for a modulation of the pump current. The solid blue line depicts the response of the ML laser output power with beam depletion control via 4 passes on the thin disk, the dash-dotted yellow curve the response of the ML laser to a simultaneous modulation of the pump power and 4-pass power for depletion control.

(100 W) required for mode-locked (ML) operation, a peak arises at 43 kHz in the amplitude of the transfer function, which results from the laser relaxation frequency. A similar measurement for the modulation of the depletion beam to the laser operating in CW has not been performed. Different spatial properties (M^2, waist, divergence) of the laser beam between CW and ML operations would have required an adaptation of the design of the imaging telescopes and beamline, which was optimized for the pulsed case. The transfer function for the pulsed 3 W control beam after passing through the AOM can be seen in dashed grey. In ML operation, the phase shift achieved for pump power modulation (with the V-I converter) is indistinguishable from that obtained for a modulation of the external beam sent onto the thin disk, both leading to a phase shift of $-90°$at 10 kHz (Fig. 2(b)). The absolute phase achieved for a modulation of the depletion beam is offset by 180° compared to the case of pump power modulation, but this offset was removed in the graph for a better visualization of the overlap. Furthermore, the magnitude of the change of f_{CEO} with the power of the controlling laser beam was measured to be 430 kHz/W at low modulation frequencies for a single pass. The 3 W laser output power used to implement the depletion modulation (reduced to an effective power of 1.5 W at the initial operating point of 50% diffraction efficiency of the AOM) provides a high tuning range to acquire the lock and ensure its proper long-term operation. The measured tuning coefficient depends on several factors including the overlap of the control beam in the gain region. Modulating the laser output using both techniques, the V-I converter and the AOM, with similar conditions, resulted in the same frequency response and bandwidth (Fig. 2 yellow dash-dot). No perturbation of the mode-locking operation was observed when the modulating beam was shone on the thin disk. Furthermore we expect that the relative intensity noise of the laser output to not be increased by the control beam. The relative power difference of two orders of magnitude between the control and intracavity beams means that the noise is dominated by the intracavity power. In addition, we expect the control beam to have a counteraction effect onto the laser intensity noise for frequencies lower than 10 kHz (as the gain is reduced for an increasing amplitude of the control beam, lowering gain and laser output power). For higher frequencies, the low-pass behaviour of the laser system further attenuates the noise by more than 10 dB.

Actively manipulating the optical power of an auxiliary CW laser interacting with the gain medium to control the intracavity power of a mode-locked laser and subsequently the CEO frequency was previously demonstrated by two different approaches leading to an enhanced modulation bandwidth that circumvented the limitation of gain modulation [21], [22], usually attributed to the upperstate lifetime of the laser transition. However, in closer inspection, the system using the co-doped Er:Yb:glass gain medium [21] has a very distinct pumping scheme where the bandwidth enhancement was achieved by bypassing the relatively slow energy transfer between the Yb and Er ions. In the case of the cross-gain modulation of a fiber laser [22], the very different cavity dynamics and parameters do not allow for a clear comparison with our system.

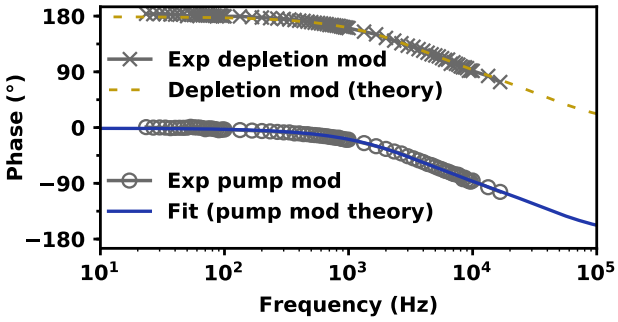

Fig. 3. Experimental and theoretical phase response of the presented system. The experimental points are for pump modulation (grey open circles) and depletion modulation (grey crosses). The pump modulation data is fitted to determine the values of q_s and $\partial q/\partial E_s$ of Eq. (18) in Ref. [23] (solid blue). The obtained parameters are used to model the response of the system for the depletion modulation via Eq. (4) (dashed yellow).

Following the derivations presented by Matos and co-workers [23], it appears that the laser needs to operate by far above threshold and the field of the modulation beam should be comparable to the intracavity field to achieve an enhancement of the control bandwidth. The derivation of a model describing the depletion modulation is presented in the Appendix. One of the important terms describing the two pole transfer function of Eq. (4) is the pump parameter r' defined as:

$$r' = 1 + \frac{\tau_L E_{pulse}}{T_R E_{sat}}(1+\delta) \tag{1}$$

where T_R is the cavity roundtrip time and τ_L the upperstate lifetime. The saturation energy of the system is E_{sat}, $\delta = \varepsilon_{mod}/E_{pulse}$ is the ratio between the energies of the modulation light and the intracavity pulse. The modeled laser response under depletion modulation shows an excellent agreement with the experimental transfer functions as shown in Fig. 3. A fit to the experimental data obtained for pump modulation was first performed with the function derived in Ref. [23] to determine the terms related to the saturable absorber. When using all parameters in the newly derived Eq. (4) for depletion modulation, one notices that it does not provide any enhancement of the modulation bandwidth in the present configuration, while perfectly matching the experimental points. The poles of Eq. (4) are highly affected by the variable r' and δ that are paramount for an increase of the effective modulation bandwidth of the system. Due to the high saturation energy of thin-disk lasers, it is challenging to achieve values of r' in the range of tens or even hundreds, which can be the case for fiber lasers. One must also take into account that the saturable losses can change drastically for different mode-locking schemes and also strongly influence the position of the poles [11]. A general rule of thumb is that a bandwidth increase requires high values of r', where the effects of ϵ are enlarged, also reducing the need of a high-energy content in the modulation beam. The unpractical scaling of δ would be the second way of improving the control capabilities. The laser reported here was run solely at an $r' \sim 2$, explaining why the observed depletion modulation bandwidth does not differ from the measured pump modulation bandwidth as this is the lowest bound for the control bandwidth of a depletion channel. Another argument supporting the measured bandwidth lies in the energy structure of Yb:YAG [24]. Modulating the zero-phonon pump line or the lasing transition affects the same energy level (depending on the inversion value). Note that the transfer function of the depletion beam power (Fig. 2(a) dashed grey) also shows that the bandwidth is not limited by the electronics or the AOM.

An investigation of the effect of the number of depletion passes on the disk was also performed. The ratio between the modulation amplitude of the laser output power at 100 Hz for four and two passes on the thin disk for different control powers up to 3 W stayed constant at the value of 2. As expected from a TDL, no saturation effect was observed. This also shows that the modulation depth for a given (low) incident power increases linearly with the number of passes. Based on

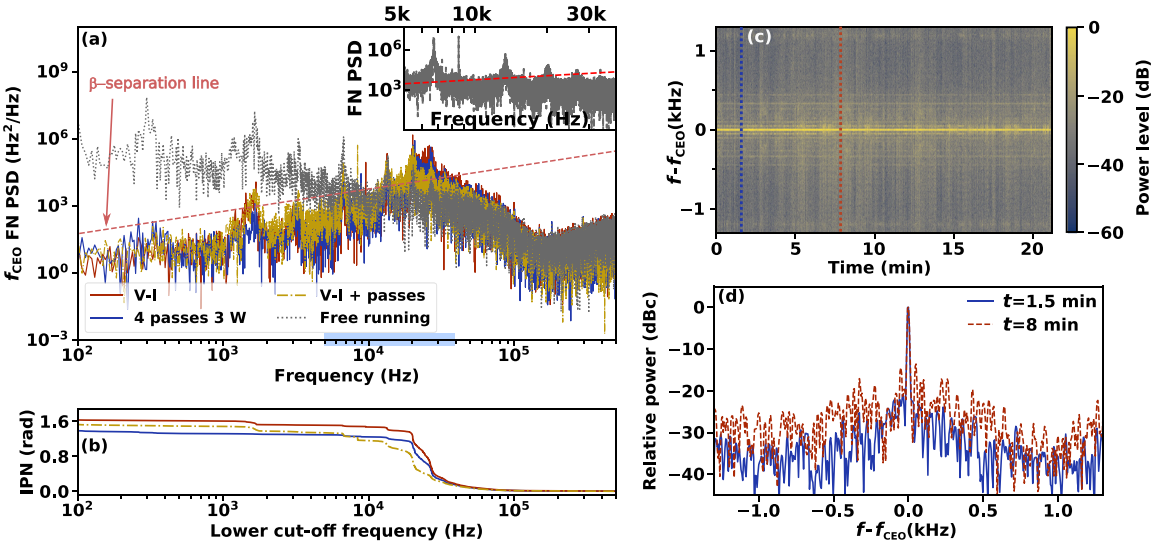

Fig. 4. Performance of the free-running and f_{CEO} locked TDL. In (a), the FN PSD of the free-running (grey dotted) beat signal is accompanied by the FN PSD of the system locked by pump control (red solid), by control of the depletion (3 W, four passes, solid blue), and for both methods simultaneously applied (yellow dash-dotted). The inset depicts an enlarged view of the free-running noise to show the 6.7 kHz peak and its harmonics, the covered range is highlighted by a shade on the x-axis of the main plot. In (b) the integrated phase noise (IPN) is shown for the three locked cases with the same color code as in (a). The IPN is 1.6 rad, 1.4 rad and 1.5 rad for pump modulation, depletion modulation and both applied simultaneously, respectively (integrated from 100 Hz to 500 kHz). (c) depicts a time series spectrogram of the locked f_{CEO} via the depletion method. The RF resolution bandwidth is 3 Hz. In (d) RF distribution cuts at $t = 1.5$ min (solid blue) and $t = 8$ min (dashed red), both marked in the spectrogram via colored dotted lines.

the extensive work showing the close relationship between laser output modulation and f_{CEO} modulation (e.g. Fig. 11 of the work by Emaury and co-workers shows a 1:1 relationship [11]), we expect the increase of amplitude to also be linearly transferred to the f_{CEO} modulation. This property enables this method to be implemented even with a low power of the control beam, to maximize the useful laser output power or when using an un-optimized AOM with a low diffraction efficiency. Additionally, a parallelization of the scheme can be envisaged, using more than one modulated beam if the required modulation power is larger than the damage threshold of a single AOM. In any case, the typical response time of the stabilization is considerably longer than any delays that a parallel approach might entail, meaning that the correspondingly induced phase shifts would be negligible for arbitrary ($\ll\mu$s) arrival delays of the different beams.

2.2 Free-Running Noise and Locked Performance

The frequency noise power spectral density (FN PSD) of the detected f_{CEO} in free-running and locked operation is depicted in Fig. 4(a). All FN PSD measurements were obtained following the method described in Ref. [15]. The inset of Fig. 4 displays the measured free-running noise at higher resolution in the frequency range between 5 kHz and 39 kHz. It shows a strong noise peak at 6.7 kHz and its 5th harmonic is still above the β-separation line [25], meaning that a feedback bandwidth of $>$30 kHz would be needed to achieve a tight CEO lock. This peak and its harmonics seem to be observed in several TDLs reported in the literature – they are present in a Yb:CALGO TDL system [11] and in a Yb:LuO TDL [13]. Similar peaks can also be observed in the stabilized CEO signal in Ref. [16], and although harmonics are barely distinguishable in the results reported in [3], [15], there is a pronounced contribution to the integrated phase noise at $\sim$7 kHz. We did not investigate the origin of these noise peaks, however it was previously

suggested that they might arise from the power supply of the pump diode, as they are clearly visible in its relative intensity noise [11]. Moreover, by stabilization of the laser average power – via a low-frequency ($<$5 kHz) feedback loop acting on the PSU – the frequency fluctuations of f_{CEO} were simultaneously reduced, but a low-frequency drift was observed, with frequency excursions of $>$2 MHz that followed the temperature of the cooling water applied to the thin disk with a slope of 3.4 MHz/K. Consequently, measures were taken to stabilize the water temperature to within 50 mK via a home-built thermo-electrically-cooled chamber. Additionally, the flow of the cooling water was reduced to 1.2 L/min while using a water cooler whose pump seems to display lower mechanical noise (Huber Minichiller 300). Before these changes no locking of f_{CEO} was possible. Despite these improvements, our system still remains noisier than other TDLs reported in the literature. Maybe lower water flows/pressure would help further, but we did not decrease the water flow past this point to avoid potential damage of the disk.

The achieved frequency noise in locked operation is very similar for all investigated feedback methods and a coherent peak was observed in the spectrum of f_{CEO} but with a limited relative power. The noise occurring in the frequency range of 10 kHz to 40 kHz remains above the β-separation line [25] and has the largest contribution to the integrated phase noise (IPN) as shown in Fig. 4(b). The small differences in IPN observed between the three locking concepts is not representative of a real difference between the methods, but result instead from small differences in the operation conditions of the TDL at the time of these measurements. Despite these fluctuations, the IPN lies consistently around 1.5 rad, corresponding to a relative power in the coherent peak in the range of 10%. With the depletion control using a 3 W beam with four passes on the disk, it was possible to maintain a stable lock for longer than 40 min, with an exemplifying spectrogram shown in Fig. 4(c) and in (d) two cuts (at times $t = 1.5$ min and $t = 8$ min). These serve to show how the changing free-running noise also influences the locking. In the f_{CEO}-locked state a decrease in amplitude noise of the system has been observed [13], [16].

We compare the present results with those reported for a Yb:LuO TDL using the same V-I converter, where a sub-radian IPN was achieved [13]. A similar low IPN should be achievable by applying the depletion technique to this Yb:LuO system. The reduced locking performance obtained with our laser results from its higher free-running noise. Achieving a lower IPN in our laser would require a reduction of its initial (free-running) noise, but can be further improved with the use of a phase-lead filter in the stabilization loop [15] and/or an active $f - 2f$ interferometer [26]. Low sub-radian IPNs might then be reached.

In the case of this particular locking scheme, in order to improve the locking times and/or performance a slow feedback loop offering a broader tuning range can be added to the system to prevent saturation of the integral term or equivalent pulling range of the feedback.

Lastly, as systems approach half a gigawatt of peak power and pulse durations of a few cycles, locking f_{CEO} to zero is also a desirable feature as it leads to emitted pulses with an identical electrical field distribution. With the f_{CEO} detection scheme used here, an AOM could be used to frequency-shift the 5.7 W beam launched into the compressor in order to lock the CEO frequency of the main laser output beam to zero [27]. Oscillators driving high-harmonic generation similarly to [28], [29] could then produce isolated attosecond pulses (using appropriate schemes) for attosecond streaking experiments [30].

3. Conclusion

In conclusion, we presented a new scheme for the f_{CEO} stabilization of TDLs and a theoretical model predicting the frequency response of the system. The method uses the large solid angle through which the gain region of a thin disk can be accessed to shine a modulated fraction of the laser output power itself. This pushes the required components beyond the detection electronics and amplifiers to solely an AOM. The modulated beam drives stimulated emission and partially depletes the inversion of the gain medium, effectively transferring the modulation to the intracavity pulse power. This self-contained technique for f_{CEO} locking is equivalent to pump modulation in terms of achievable modulation bandwidth. This constitutes the proof of principle of an alternative

locking scheme capable of similar performance as pump modulation, e.g., to yield sub-radian IPNs for systems displaying low enough noise figures in free-running mode.

Appendix

In our model, Eq. (15) of reference [23] is modified by adding the energy ε of the auxiliary modulated beam shining onto the gain medium as follows:

$$T_R \frac{dg}{dT} = -\frac{g - g_0}{\tau_L / T_R} - g\frac{E + \varepsilon}{E_{sat}} \tag{2}$$

where g is the time dependent gain with g_0 the small signal gain, and E represents the energy of the intracavity pulse. The time coordinate is represented by T to emphasize the fact that the changes occur over timescales much larger than the roundtrip time, possible for solid-state lasers with long upperstate lifetimes. After linearisation, an equation of the form of Eq. (17) in Ref. [23] is obtained (neglecting the pump modulation term):

$$T_R \frac{d\Delta g}{d\Delta T} = -r' \frac{T_R}{\tau_L} \Delta g - \frac{g_s}{E_{sat}} (\Delta E + \Delta \varepsilon). \tag{3}$$

The Δ symbol indicates the new linearized variables. Algebric manipulations were done following the guidelines presented in Ref. [23] to derive a model for the response of the system to a modulated depletion energy ε:

$$\frac{\tilde{E}}{\tilde{\varepsilon}} = \frac{-(l + q_s)/E_{sat}}{s^2 + \left(\frac{r'}{\tau_L} + \frac{\partial g}{\partial E_s} P_s\right) s + P_s \frac{\partial g}{\partial E_s} \frac{r'}{\tau_L} + \frac{r'-1}{\tau_L T_R} (l + q_s)} \tag{4}$$

where the tilde symbol represents the variables in Laplace space and s is the Laplace complex frequency. The steady state effective saturable absorber loss due to mode-locking is q_s and $\partial q / \partial E_s$ is its first derivative as a function of energy at the steady state. Lastly, l represents the system losses.

References

[1] J. Brons *et al.*, "Energy scaling of Kerr-lens mode-locked thin-disk oscillators," *Opt. Lett.*, vol. 39, no. 22, pp. 6442–6445, Nov. 2014.

[2] C. J. Saraceno, D. Sutter, T. Metzger, and M. Abdou Ahmed, "The amazing progress of high-power ultrafast thin-disk lasers," *J. Eur. Opt. Soc.-Rapid Publications*, vol. 15, no. 1, Jun. 2019, Art. no. 15.

[3] O. Pronin *et al.*, "High-power multi-megahertz source of waveform-stabilized few-cycle light," *Nature Commun.*, vol. 6, May 2015, Art. no. 6988.

[4] K. F. Mak *et al.*, "Compressing μ J-level pulses from 250 fs to sub-10 fs at 38-MHz repetition rate using two gas-filled hollow-core photonic crystal fiber stages," *Opt. Lett.*, vol. 40, no. 7, pp. 1238–1241, Apr. 2015.

[5] M. Krebs *et al.*, "Towards isolated attosecond pulses at megahertz repetition rates," *Nature Photon.*, vol. 7, no. 7, pp. 555–559, Jul. 2013.

[6] I. Coddington, N. Newbury, and W. Swann, "Dual-comb spectroscopy," *Optica*, vol. 3, no. 4, pp. 414–426, Apr. 2016.

[7] M. C. Stowe *et al.*, "Direct frequency comb spectroscopy," in *Advances In Atomic, Molecular, and Optical Physics*, E. Arimondo, P. R. Berman, and C. C. Lin, Eds, vol. 55. New York, NY, USA: Academic, Jan. 2008, pp. 1–60.

[8] D. J. Jones *et al.*, "Carrier-envelope phase control of femtosecond mode-locked lasers and direct optical frequency synthesis," *Science*, vol. 288, no. 5466, pp. 635–639, 2000.

[9] H. Telle, G. Steinmeyer, A. Dunlop, J. Stenger, D. Sutter, and U. Keller, "Carrier-envelope offset phase control: A novel concept for absolute optical frequency measurement and ultrashort pulse generation," *Appl. Phys. B*, vol. 69, no. 4, pp. 327–332, Oct. 1999.

[10] J. M. Dudley, G. Genty, and S. Coen, "Supercontinuum generation in photonic crystal fiber," *Rev. Modern Phys.*, vol. 78, no. 4, pp. 1135–1184, Oct. 2006.

[11] F. Emaury *et al.*, "Frequency comb offset dynamics of SESAM modelocked thin disk lasers," *Opt. Exp.*, vol. 23, no. 17, pp. 21 836–21 856, Aug. 2015.

[12] A. Klenner *et al.*, "Phase-stabilization of the carrier-envelope-offset frequency of a SESAM modelocked thin disk laser," *Opt. Exp.*, vol. 21, no. 21, pp. 24 770–24 780, Oct. 2013.

[13] N. Modsching *et al.*, "Carrier-envelope offset frequency stabilization of a thin-disk laser oscillator operating in the strongly self-phase modulation broadened regime," *Opt. Express*, vol. 26, no. 22, pp. 28461–28468, Oct. 2018.

[14] C. J. Saraceno *et al.*, "Self-referenceable frequency comb from an ultrafast thin disk laser," *Opt. Exp.*, vol. 20, no. 9, pp. 9650–9656, Apr. 2012.
[15] M. Seidel *et al.*, "Carrier-envelope-phase stabilization via dual wavelength pumping," *Opt. Lett.*, vol. 41, no. 8, pp. 1853–1856, Apr. 2016.
[16] S. Gröbmeyer, J. Brons, M. Seidel, and O. Pronin, "Carrier-envelope-offset frequency stable 100 W-level femtosecond thin-disk oscillator," *Laser Photon. Rev.*, vol. 13, no. 3, 2019, Art. no. 1800256.
[17] F. Ö. Ilday, D. K. Kesim, M. Hoffmann, and C. J. Saraceno, "Discrete similariton and dissipative soliton modelocking for energy scaling ultrafast thin-disk laser oscillators," *IEEE J. Sel. Topics Quantum Electron.*, vol. 24, no. 5, pp. 1–12, Sep. 2018.
[18] K. Gürel, S. Schilt, and T. Südmeyer, "Carrier-envelope offset frequency stabilization of a fiber laser by cross gain modulation," *IEEE Photon. J.*, vol. 10, no. 2, Apr. 2018, Art. no. 3200306.
[19] M. Bradler, P. Baum, and E. Riedle, "Femtosecond continuum generation in bulk laser host materials with sub-μJ pump pulses," *Appl. Phys. B*, vol. 97, no. 3, pp. 561–574, Aug. 2009.
[20] L. Xu, T. W. Hänsch, C. Spielmann, A. Poppe, T. Brabec, and F. Krausz, "Route to phase control of ultrashort light pulses," *Opt. Lett.*, vol. 21, no. 24, pp. 2008–2010, Dec. 1996.
[21] L. Karlen, G. Buchs, E. Portuondo-Campa, and S. Lecomte, "Efficient carrier-envelope offset frequency stabilization through gain modulation via stimulated emission," *Opt. Lett.*, vol. 41, no. 2, pp. 376–379, Jan. 2016.
[22] K. Gürel, S. Hakobyan, V. J. Wittwer, S. Schilt, and T. Südmeyer, "Frequency comb stabilization of ultrafast lasers by opto-optical modulation of semiconductors," *IEEE J. Sel. Topics Quantum Electron.*, vol. 24, no. 5, Sep. 2018, Art. no. 1102309.
[23] L. Matos, O. D. Mücke, J. Chen, and F. X. Kärtner, "Carrier-envelope phase dynamics and noise analysis in octave-spanning Ti:sapphire lasers," *Opt. Exp.*, vol. 14, no. 6, pp. 2497–2511, Mar. 2006.
[24] J. Koerner *et al.*, "Measurement of temperature-dependent absorption and emission spectra of Yb:YAG, Yb:LuAG, and Yb:CaF_2 between 20 °C and 200 °C and predictions on their influence on laser performance," *JOSA B*, vol. 29, no. 9, pp. 2493–2502, Sep. 2012.
[25] G. D. Domenico, S. Schilt, and P. Thomann, "Simple approach to the relation between laser frequency noise and laser line shape," *Appl. Opt.*, vol. 49, no. 25, pp. 4801–4807, Sep. 2010.
[26] R. Liao, H. Tian, T. Feng, Y. Song, M. Hu, and G. Steinmeyer, "Active F-to-2F interferometer for record-low jitter carrier-envelope phase locking," *Opt. Lett.*, vol. 44, no. 4, pp. 1060–1063, Feb. 2019.
[27] S. Rausch, T. Binhammer, A. Harth, E. Schulz, M. Siegel, and U. Morgner, "Few-cycle oscillator pulse train with constant carrier-envelope- phase and 65 as jitter," *Opt. Exp.*, vol. 17, no. 22, pp. 20 282–20 290, Oct. 2009.
[28] F. Emaury, A. Diebold, C. J. Saraceno, and U. Keller, "Compact extreme ultraviolet source at megahertz pulse repetition rate with a low-noise ultrafast thin-disk laser oscillator," *Optica*, vol. 2, no. 11, pp. 980–984, Nov. 2015.
[29] F. Labaye *et al.*, "Extreme ultraviolet light source at a megahertz repetition rate based on high-harmonic generation inside a mode-locked thin-disk laser oscillator," *Opt. Lett.*, vol. 42, no. 24, pp. 5170–5173, Dec. 2017.
[30] J. Itatani, F. Quéré, G. L. Yudin, M. Y. Ivanov, F. Krausz, and P. B. Corkum, "Attosecond streak camera," *Phys. Rev. Lett.*, vol. 88, no. 17, Apr. 2002, Art. no. 173903.